



Analysis and representation of non-stationary signals in inertia-reduced power grids

Prof. Mario Paolone
EPFL Distributed Electrical Systems Lab

Invited seminar at ETHZ
03.10.2022

Contributors

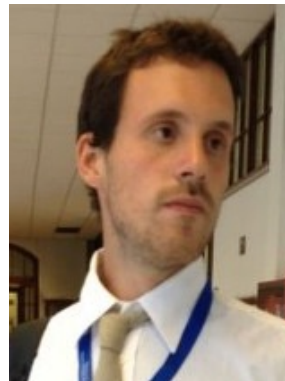
Prof. Mario Paolone



Alex Karpilow



Dr. Guglielmo Frigo
(Metas)



Dr. Asja Derviškadić
(Swissgrid)



The context

- Power systems are **large, nonlinear, multi-time-scale, discrete/continuous complex systems**.
- Usually analyzed for specific problems with relatively simplified models under appropriate assumptions, e.g.
 - Dynamics (electromechanical) dominated by the **response of synchronous machines** → use of **time-varying phasors**.
 - **Electromagnetic transient models** when **time-varying phasors** are not **appropriate**.
- The increased penetration of **converter-interfaced generation (CIG)** and **HVDC** in power systems **challenges the above decomposition of power system studies into phasor-based vs electromagnetic-transient-based**.
- New needs in dynamics, control and stability studies of systems with significant penetration of CIG.

The context

Event of September 28, 2016, Australia

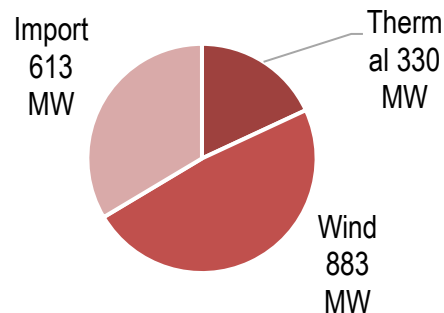
Multiple tornadoes in South Australia (SA) tripped multiple 275 kV transmission circuits, and resulted in multiple faults in quick succession.

The series of voltage dips from the faults triggered protection on several wind farms to runback about 456 MW of wind generation.

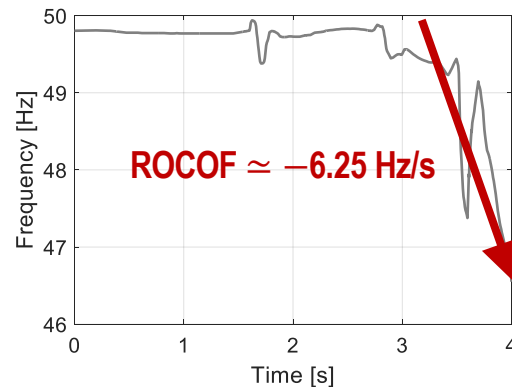
The reduction in wind farm output was compensated by an increase in power imported from Victoria. However, the import reached a level that tripped the interconnector on loss of synchronism protection.

The loss of power infeed from the wind farms and import from Victoria resulted in the frequency falling so fast that load shedding schemes were unable to stop the fall, resulting in a blackout.

SA pre-black-out generation mix



System frequency

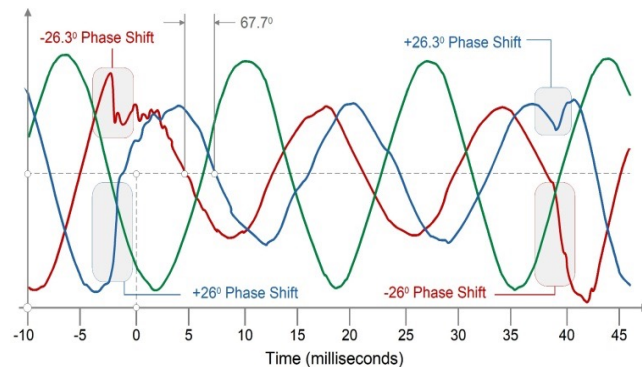
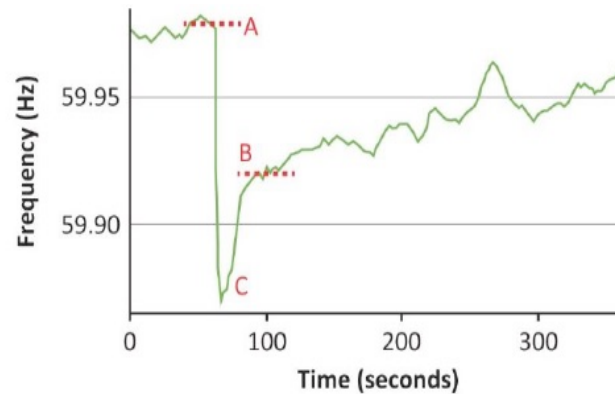


The context

Event of August 16, 2016, California

A fault induced a total of 1'178 MW of PV power interruption.

- The majority of inverters trip instantaneously based on frequency measurements obtained from PLLs; it was determined that these inverters are susceptible to erroneous tripping due to frequency changes; this response accounted for **700 MW of the lost generation**.
- A number of inverters that tripped were configured to **cease current injection if the voltage goes above 1.1 pu or below 0.9 pu**; the inverters were returned to pre-disturbance level at a slow ramp rate; this response accounted for about **450 MW of lost generation**.



The consequences

- Summary of use cases for frequency and ROCOF
 - **Loss of Mains (LOM)** protection
 - Isolation of network areas (due to maintenance or faults) can pose security risks to personnel from intermittent unexpected voltages
 - LOM (anti-islanding) relays, used to **disconnect local renewables**, are notorious for false trips (noise sensitivity of ROCOF, system disturbances)
 - **Under Frequency Load Shedding (UFLS)** applications
 - Last resort protection scheme to **disconnect loads** for frequency maintenance
 - False tripping can trigger other UFLS schemes and result in widespread loss of load and over frequency events
- False triggering
 - Phase/amplitude steps (due to network configuration, circuit breaker operations, remote faults) can trigger these protection schemes.

Adequacy of signal processing techniques

Traditional power system analysis deals with signals approximated as quasi-stationary sinusoids. In the frequency-domain, such signals are characterized by **narrow spectral bandwidth**.

- **Narrow-band signals:** discrete spectrum with energy concentrated around a single sinusoidal component.

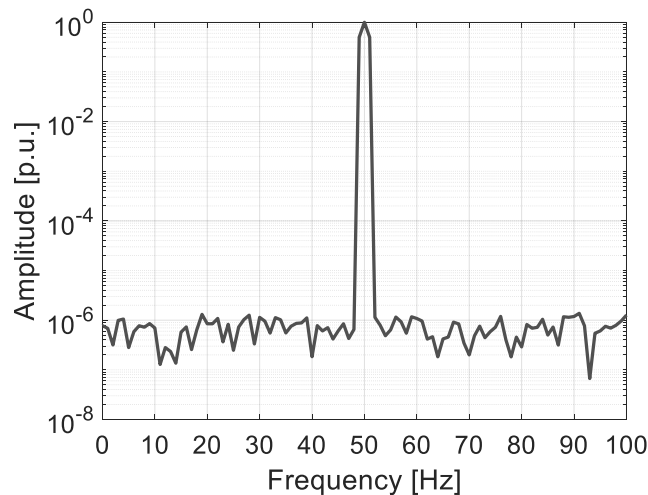
In reduced-inertia power grids, signals representative of voltages and/or currents may experience fast variations that may violate this assumption. In the frequency-domain, the energy of these signals occupies a broader bandwidth.

- **Broad-band signals:** continuous spectrum of generic bandwidth → **spectrum of the signal (and its energy) cannot be reconstructed by a finite set of sinusoidal components.**

Adequacy of signal processing techniques

Steady-state

$$v(t) = A \cdot \cos(2\pi f t)$$

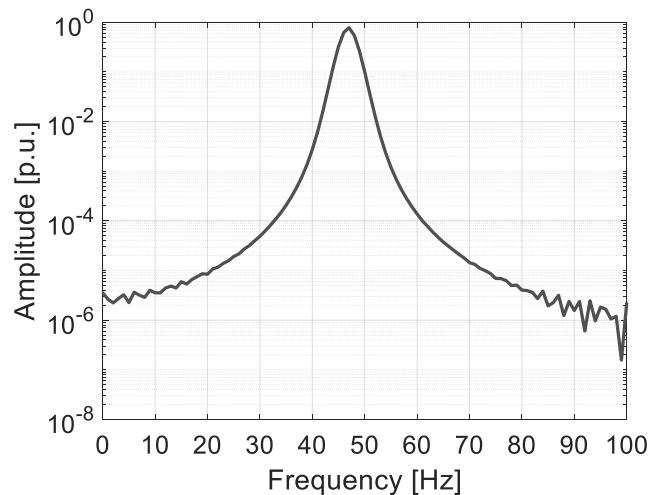


Energy of the signal in [48, 52] Hz
99.X%

→ **Narrow-band signal**

Transient with ROCOF $R=-6.25$ Hz/s

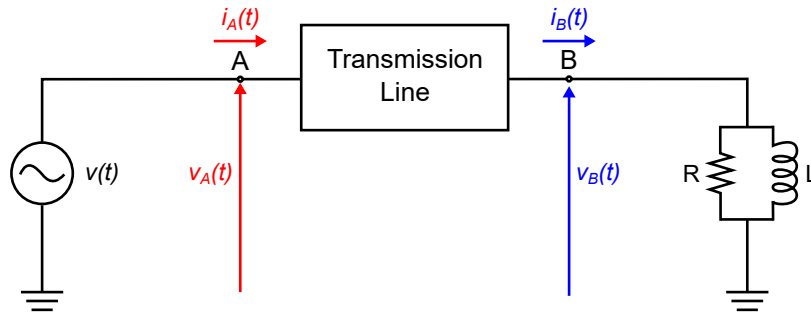
$$v(t) = A \cdot \cos(2\pi(f + Rt)t)$$



Energy of the signal in [48, 52] Hz
32%

→ **Broad-band signal**

Adequacy of signal processing techniques



- Numerical experiment carried out using the EMTP-RV
- Voltage generator: 380 kV (ph-ph), **generic time-dependent voltage source**
- Line: 100 km frequency-dependent model
- Load: R-L parallel equivalent \rightarrow 400 MW, $\cos\varphi$ 0.9
- $v_A(t)$ **negative frequency ramp characterized by RoCoF of -5 Hz/s (starting from 50 Hz)**
- $v_A(t)$ **amplitude modulation characterized by 10% depth and 5 Hz modulating frequency**

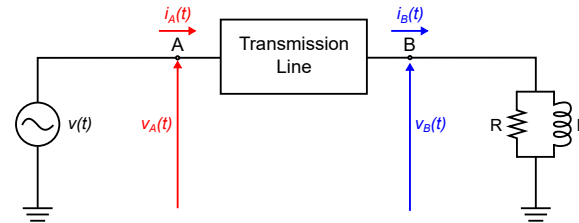
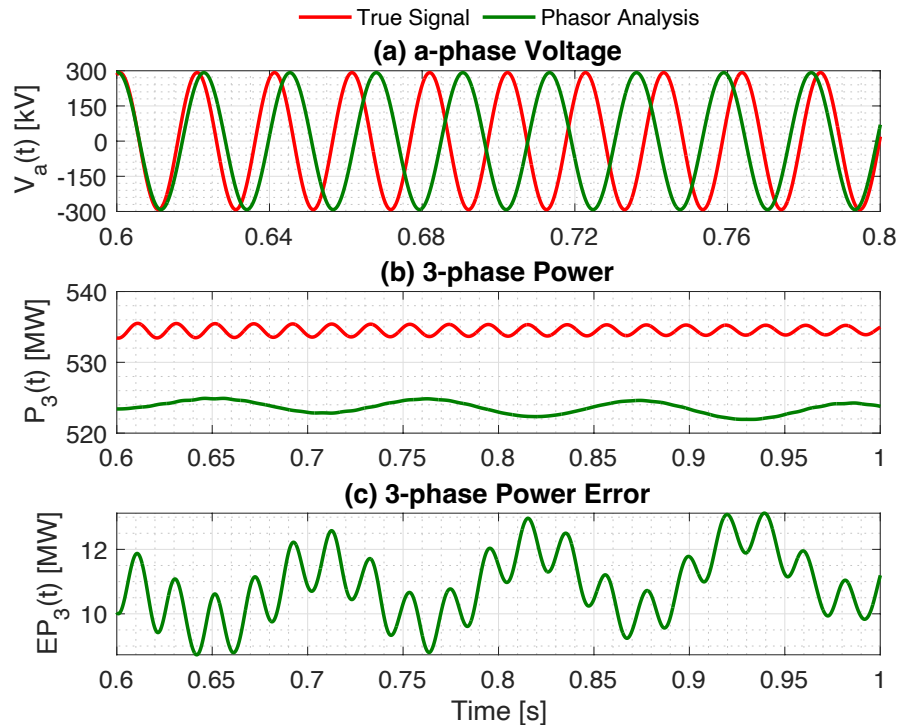
Adequacy of signal processing techniques

- Phasor analysis based on IEC Std. 61000-4-7, sliding window of 200 ms.

- 1: $p(t) = \sum_{abc} v(t) \cdot i(t)$ True instantaneous power
- 2: **for** $x(t) = \{v(t), i(t)\}_{abc}$
- 3: $\tilde{x}(t) = x(t) + \mathcal{N}(t)$ Noise adding, SNR = 80 dB
- 4: **for** $t = 0 \rightarrow end, \Delta t = 200ms, \Delta f = 5Hz$
- 5: $X(k) = \mathcal{F}[x(t) \cdot w(t)]$ Hanning window, $\mathcal{F} \approx$ DFT
- 6: $\{\tilde{f}(t), \tilde{A}(t), \tilde{\varphi}(t)\} = IpDFT[X(k)]$ Estimate of the phasor params
- 7: $\tilde{x}_{\mathcal{F}}(t) = \tilde{A}(t)\cos(2\pi\tilde{f}(t)\Delta t/2 + \tilde{\varphi}(t))$ Reconstruct the time-domain signal
- 8: **end for**
- 9: **end for**
- 10: $\tilde{p}_{\mathcal{F}}(t) = \sum_{abc} \tilde{v}_{\mathcal{F}}(t) \cdot \tilde{i}_{\mathcal{F}}(t)$ Instantaneous power of the reconstructed signals
- 11: $\Delta p_{\mathcal{F}}(t) = \tilde{p}_{\mathcal{F}}(t) - p(t)$ Power error

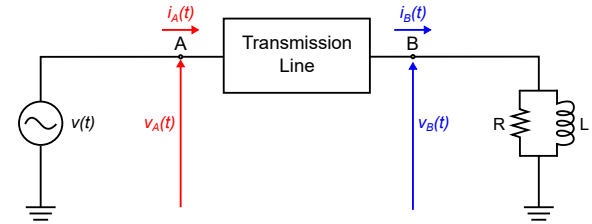
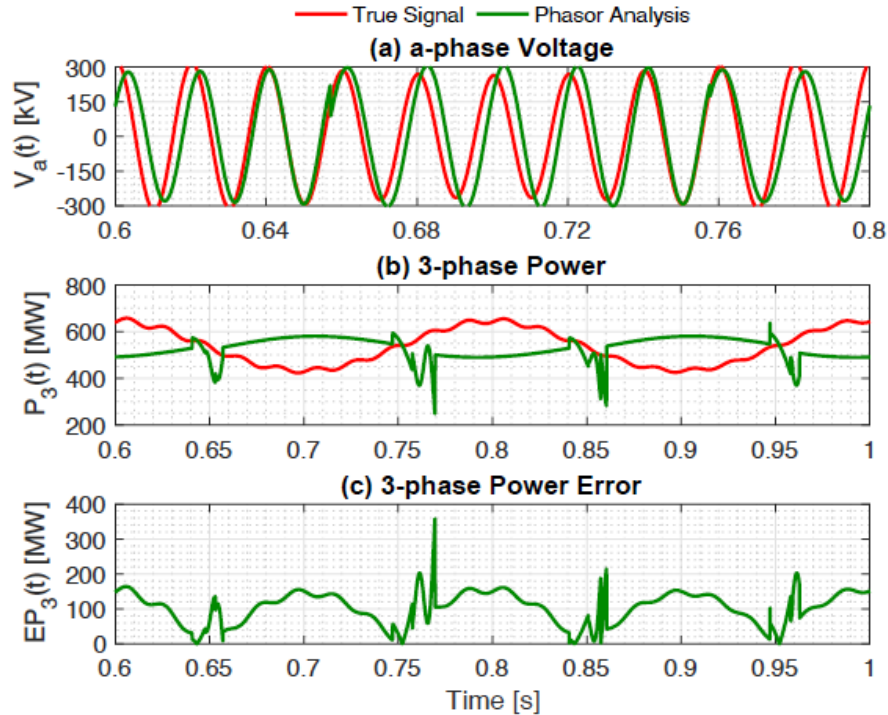
Adequacy of signal processing techniques

Frequency ramp of -5 Hz/s applied to $v_A(t)$

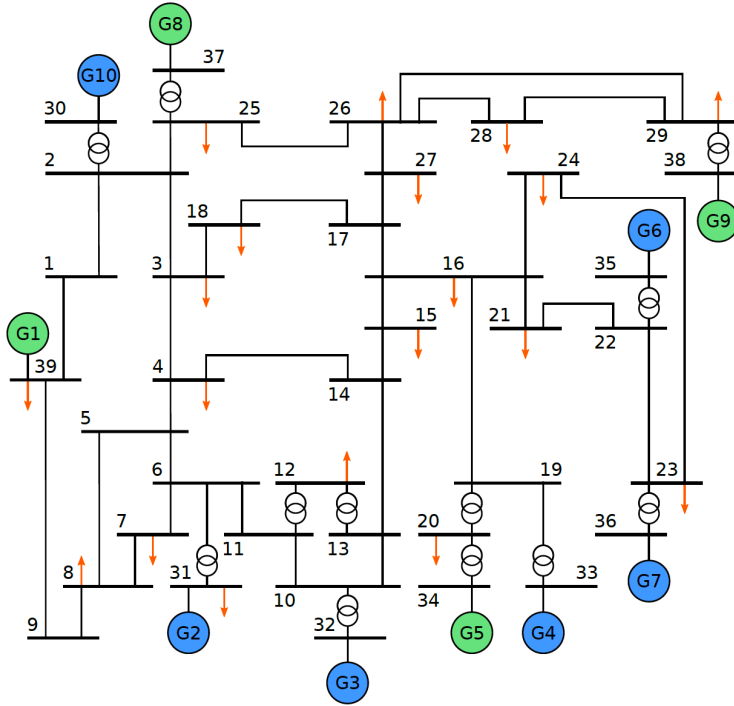


Adequacy of signal processing techniques

10% amplitude modulation with modulating frequency of 5 Hzs applied to $v_A(t)$



Adequacy of signal processing techniques

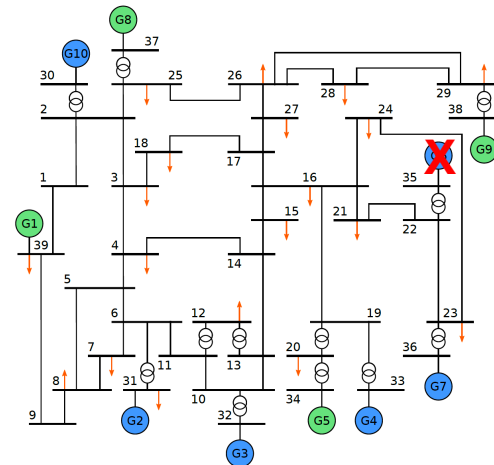
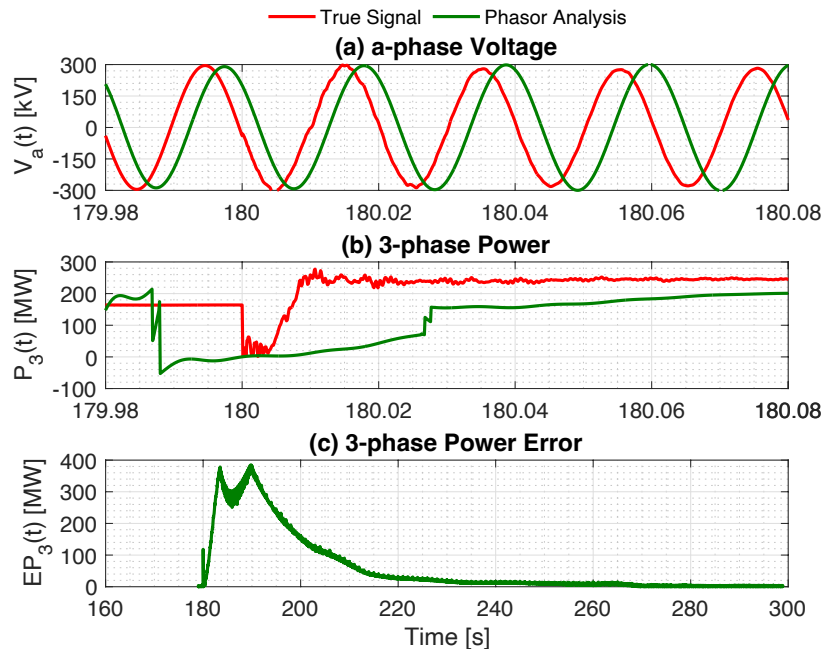


- IEEE 39-bus test system
- 345 kV
- 10 GW installed capacity
- 3 configurations:
 - I: original 10 machines
 - II: 4 wind farms (4 GW)
 - III: 4 wind farms + BESS (0.2 GW)
- Generator G6 tripped (800 MW)

[online: <https://github.com/DESL-EPFL/>]

Adequacy of signal processing techniques

Outage of generator G6 @ 180 s (800 MW), analysis for the node at bus #21



$$\Delta p_F = 400 \text{ MW}$$

Possible solutions

To overcome the **limitations of traditional phasor analysis**, two possible approaches:

- **Dynamic phasor analysis**

Dynamic phasors have been introduced as an **extension of the phasor concept**, where **fundamental parameter time-derivatives are included in the signal model**.

Enhanced signal models allow for more accurate reconstruction of time-varying parameters and **soften the stationarity constraint**. **However, it is not possible to dissociate dynamic phasor from DFT-based analysis, and they are likely to face similar model inconsistency issues.**

- **Functional basis analysis**

information theory provides several **transformations and projection bases other than simple sinusoids/complex exponentials** for the analysis of time-varying or continuous spectrum signals.

Dynamic phasors: pros & cons

- **Outperform stationary phasors** in dynamic conditions.
- Prove to be **compliant with IEEE Std requirements**.
- **Still rely on narrow-band approximations** of signals and **cannot represent** in a complete way signals characterized by a **continuous spectrum** (see comparison with Functional Basis Analysis presented next).

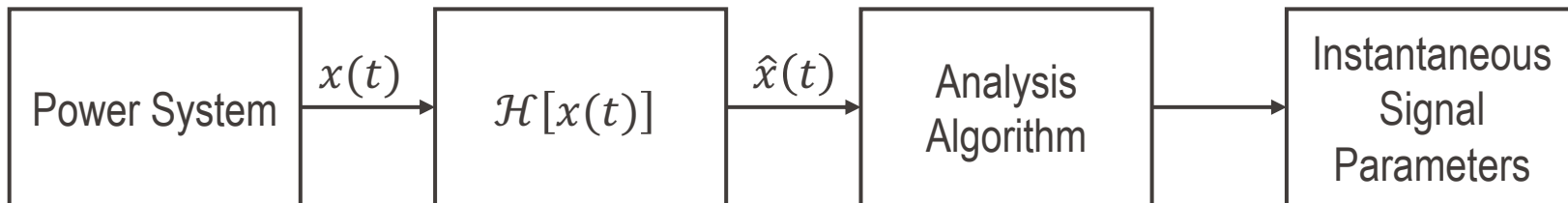
→ NEED FOR ALTERNATIVE TRANSFORMATIONS

Analysis of Broad-Band Signals in Reduced-Inertia Power Systems Using the Hilbert Transform (HT)

- As seen at the beginning of the seminar, the exact modeling of inertia-less power systems may require the use of more sophisticated representations other than phasors

Proposal: Can we project on a **different functional basis** not based on sinusoids that enables us to reconstruct the whole spectrum and, therefore, capable to **model the power transfer on the whole spectrum**?

- The **Hilbert Transform (HT)** may be the appropriate tool since its use results into negligible errors in the reconstruction of the spectral power transfer in case of extreme power systems transients



Power Systems Transients Using the HT

Given a generic time varying real signal $x(t)$, its HT is defined as:

$$\tilde{x}(t) = \mathcal{H}[x(t)] = \frac{1}{\pi} P \int_{-\infty}^{\infty} \frac{x(\tau)}{t - \tau} d\tau$$

being P the Cauchy principal value.

The real signal $x(t)$ and its HT form the so-called **analytic signal**:

$$\hat{x}(t) = x(t) + j \cdot \mathcal{H}[x(t)] = x(t) + j \cdot \tilde{x}(t)$$

About the Cauchy principal value: it is used to assign a value to the integral $\int_{-\infty}^{\infty} \frac{x(\tau)}{t - \tau} d\tau$ which would be undefined when the denominator is null.

The Cauchy p.v. is defined according to the following rule (being $f(x)$ singular at the finite number b):

$$p. v. = \lim_{\epsilon \rightarrow 0^+} \left[\int_a^{b-\epsilon} f(x) dx + \int_{b+\epsilon}^c f(x) dx \right]$$

Power Systems Transients Using the HT

- **Property 1:** the HT introduces a phase shift of $-\pi/2$ at each positive frequency and $+\pi/2$ at each negative frequency.
- **Property 2:** the HT of the product of two signals with non-overlapping spectra equals to the product of the low-pass term by the HT of the high-pass term.
- **Property 3:** the spectral representation of the analytic signal does not contain imaginary components but only real components.
- **Property 4:** the analytic signal can be considered as a generalization of the concept of phasor representation, characterized by an instantaneous frequency $f_0 = \omega_0/2\pi$.

HT applied to Power System Transients

- **Amplitude Modulation** → inter-area oscillations between large system regions

$$x(t) = A(1 + k_a \cos(2\pi f_a t)) \cos(2\pi f_0 t + \varphi_0)$$

FT

$$\begin{aligned} \mathcal{F}[x(t)] &= \\ &= \frac{A}{2} \cdot [\delta(f - f_0)e^{j\varphi_0} + \delta(f + f_0)e^{-j\varphi_0} + \frac{k_a}{2} \\ &\cdot [\delta(f - (f_0 + f_a))e^{j\varphi_0} + \delta(f + (f_0 + f_a))e^{-j\varphi_0} + \delta(f - (f_0 - f_a))e^{j\varphi_0} + \delta(f + (f_0 - f_a))e^{-j\varphi_0}] \end{aligned}$$

HT

$$\hat{x}(t) = A \cdot [1 + k_a \cos(2\pi f_a t)] \cdot e^{j(2\pi f_0 t + \varphi_0)}$$

HT applied to Power System Transients

- **Frequency Ramp** → severe system collapse

$$x(t) = A \cos(2\pi f_0 t + \varphi_0 + R\pi t^2)$$

FT

$$\mathcal{F}[x(t)] = \frac{A}{2\sqrt{R}} e^{j\left[\frac{\pi(f-f_0)^2}{R} - \frac{\pi}{4} + \varphi_0\right]} + \frac{A}{2\sqrt{R}} e^{-j\left[\frac{\pi(f+f_0)^2}{R} - \frac{\pi}{4} + \varphi_0\right]}$$

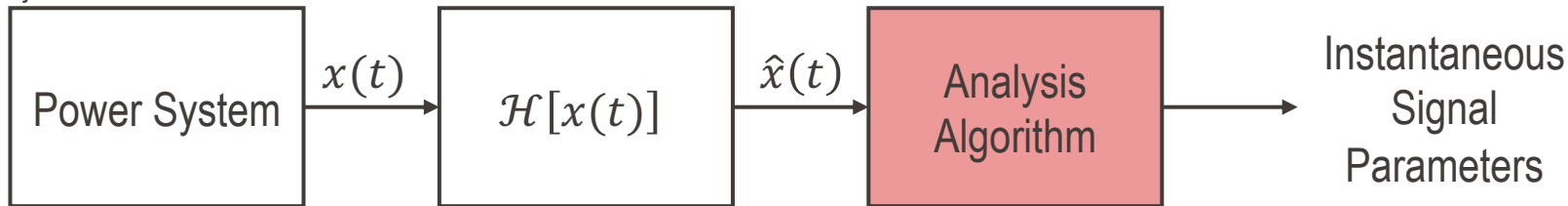
HT

$$\hat{x}(t) = A e^{j(2\pi f_0 t + \varphi_0 + R\pi t^2)}$$

HT applied to Power System Measurements

- The HT may provide an **exact match between the real-valued time-domain signal and its analytic representation**
- If we project the real-valued signal in $x(t)$ over a basis containing the analytic signal in $\hat{x}(t)$, we will obtain a projection coefficient that **may unequivocally identifies the parameters of the signal in $x(t)$.**
- **How do we engineer this functional basis in order to extract signal parameters with a high level of fidelity?**

Characterization of Non-Stationary Signals



Goal:

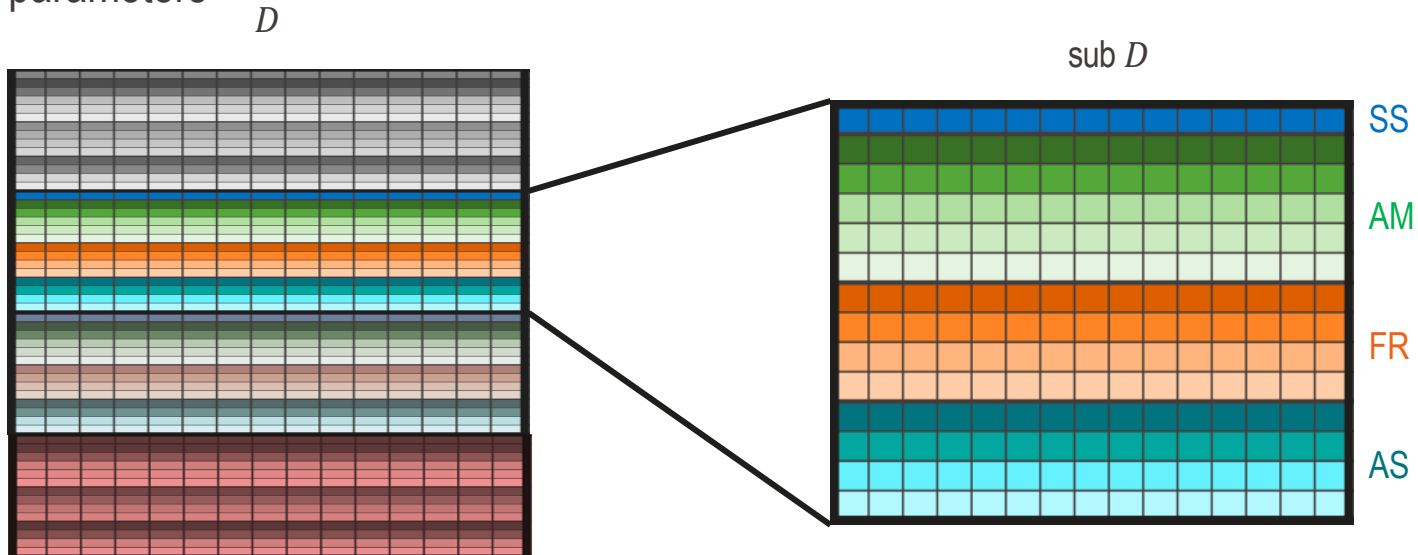
- Extracting valid signal parameters from measured signals in power grids
- Exploit improved representation of signal dynamics using Hilbert Transform

Inspired by:

- **Fourier and Wavelet analysis** which rely on bases of complex exponentials and wavelet kernels
 - **Compressed Sensing** which use dictionaries of kernels to reconstruct inputs
- **Create a suitable dictionary based on the Hilbert Transform for instantaneous signal parameter extraction.**

Dictionary Formulation

- Assumption that the set of possible signal dynamics in the grid is finite
 - Can be spanned by a dictionary of common dynamics (e.g., AM, FR, AS)
 - Dictionary is **user-engineered to capture dynamics of interest**
- Each atom in the dictionary represents a specific function for a defined set of parameters



Kernel Models

$$d = DFT \left[(1 + g_A(t)) \cdot e^{j(2\pi f_0 t + g_\varphi(t))} \right]$$

The frequency of the fundamental component is limited to a finite bandwidth between 48 and 52 Hz, for each fundamental frequency, the following vectors are included in D :

- A **steady-state (SS)** sinusoid

$$d = DFT \left[e^{j(2\pi f_0 t)} \right]$$

- A sinusoid characterized by an **Amplitude Modulation (AM)**

$$d = DFT \left[(1 + k_m \cos(2\pi f_m t + \varphi_m)) \cdot e^{j(2\pi f_0 t)} \right]$$

$$k_m = 10\%, f_m = [0,5] \text{ Hz}, \varphi_m = [0, 2\pi] \text{ rad}$$

Kernel Models

$$d = DFT \left[(1 + g_A(t)) \cdot e^{j(2\pi f_0 t + g_\varphi(t))} \right]$$

The frequency of the fundamental component is limited to a finite bandwidth between 48 and 52 Hz, for each fundamental frequency, the following vectors are included in D :

- A sinusoid characterized by a **Frequency Ramp (FR)**

$$d = DFT \left[e^{j(2\pi f_0 t + R\pi t^2)} \right]$$

$$R = [-5, 5] \text{ Hz/s}$$

- A sinusoid characterized by an **Amplitude Step (AS)**

$$d = DFT \left[(1 + k_s h_s(t - t_s)) \cdot e^{j(2\pi f_0 t)} \right]$$

$$k_s = [10, 100]\%, t_s = [0.01, T_w - 0.01] \text{ ms}$$

Kernel Models

$$d = DFT \left[(1 + g_A(t)) \cdot e^{j(2\pi f_0 t + g_\varphi(t))} \right]$$

The frequency of the fundamental component is limited to a finite bandwidth between 48 and 52 Hz, for each fundamental frequency, the following vectors are included in D :

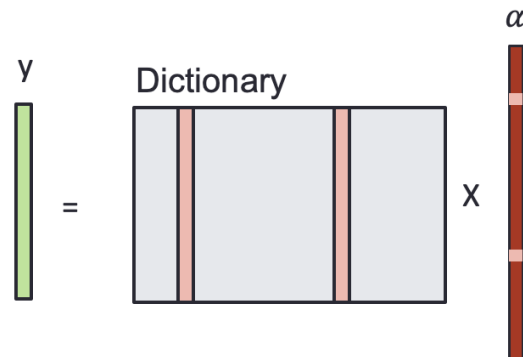
- A sinusoid characterized by a **Phase Modulation (PM)**

$$d = DFT \left[e^{j(2\pi f_0 t + k_a \cos(2\pi f_a t + \varphi_a))} \right]$$

$$k_a = 10\%, f_a = [0, 5] \text{ Hz}, \varphi_a = [0, 2\pi] \text{ rad}$$

Dictionary Design

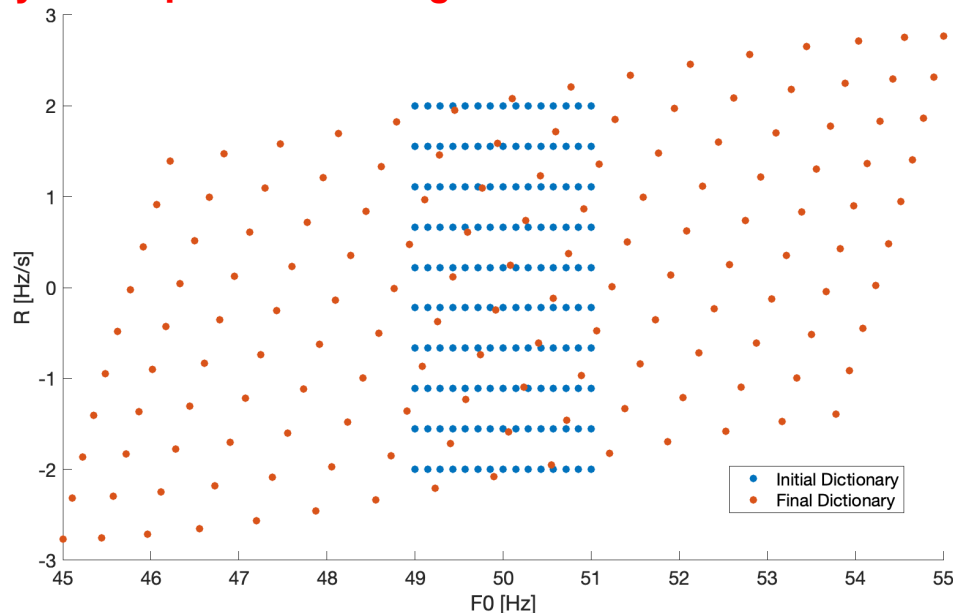
- Parameterized dictionary:
 - **Designing an optimal dictionary: what are the best parameter sets?**
 - *Compressed Sensing* involves reconstruction of signals with kernels of dictionaries
- Coherence
 - $\mu(D) = \max_{1 \leq i < j \leq n} |d_i^H d_j| / (\|d_i\|_2 \|d_j\|_2)$
 - Orthogonal basis has $\mu = 0$
 - Dictionaries are typically frames (not bases)
- Equiangular Tight Frame (ETF):
 - Frame vectors are maximally separated in space (minimum coherence)



Dictionary Design

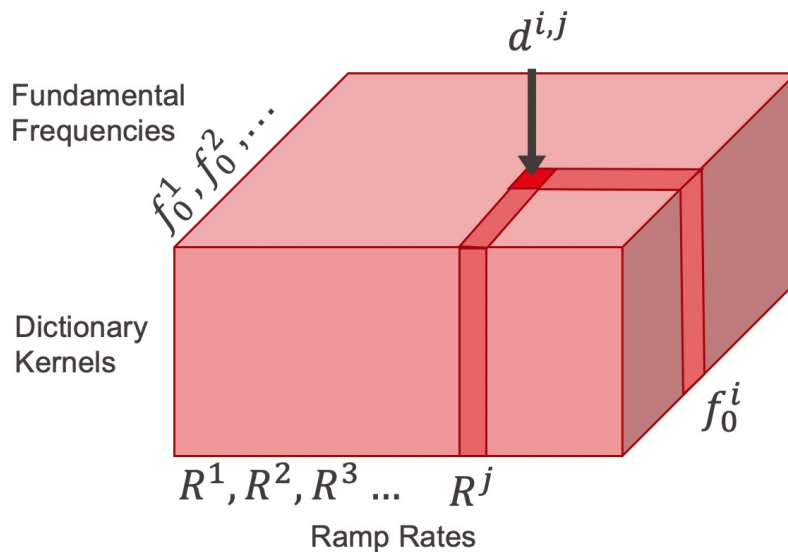
- Parametric Dictionary Design [12]
 - Optimize over parameters to minimize coherence
 - Conclusion: **dictionary coherence is minimized when kernel parameters are spread uniformly in the parameter ranges**

Frequency Ramp
Dictionary
 $D(f_0, R)$



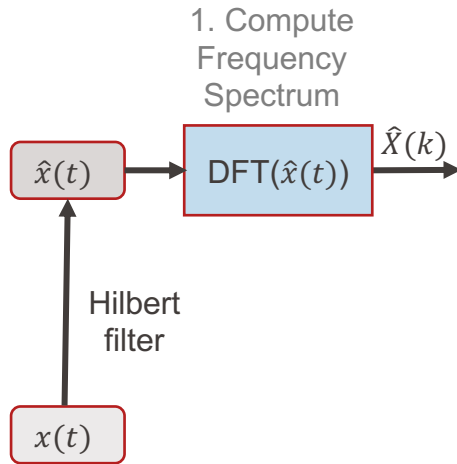
Dictionary Design

- Fixed parameter resolutions and ranges
- Kernels represent all combinations of parameters
- Tensor of rank $p+1$ for p parameters
 $D \in \mathbb{C}^{n_1 \times n_2 \times d}$
- Pre-computed dictionaries:
 - Amplitude Modulations
 - Phase Modulations
 - Frequency Ramps
 - Amplitude Steps



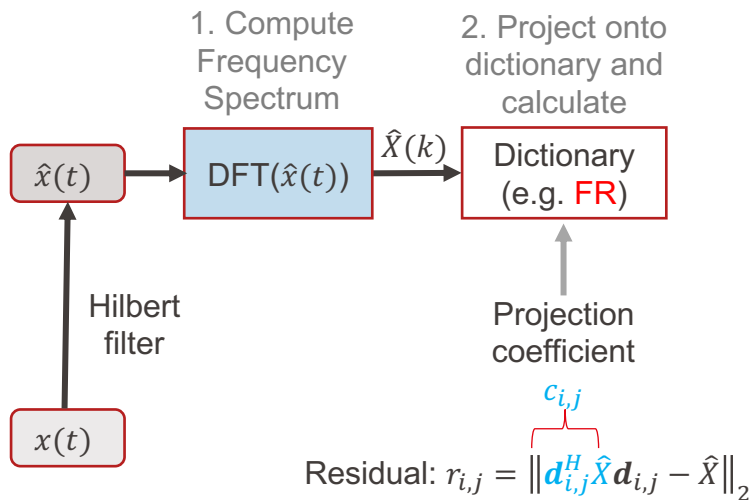
Functional Basis Analysis

- Parameter Identification



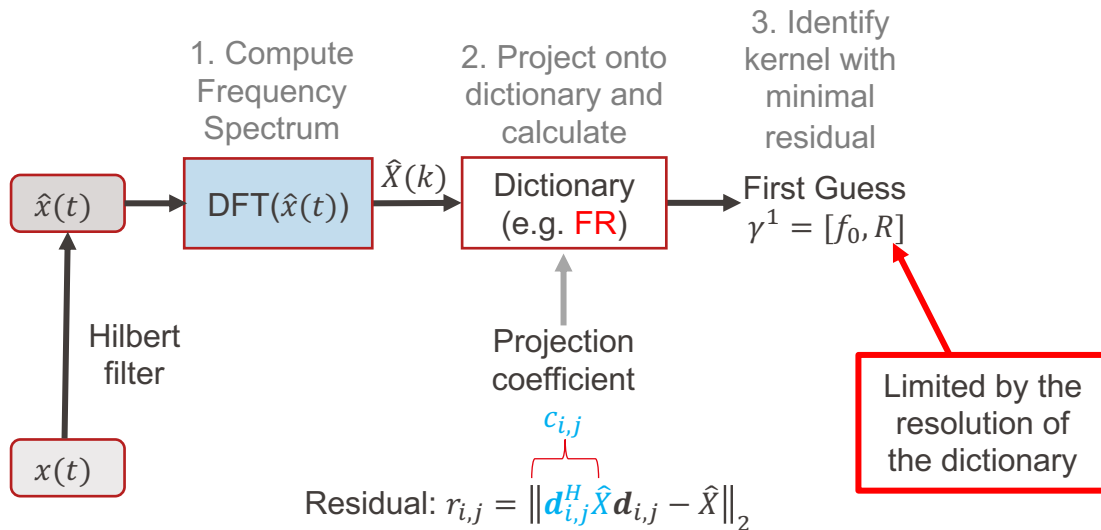
Functional Basis Analysis

- Parameter Identification



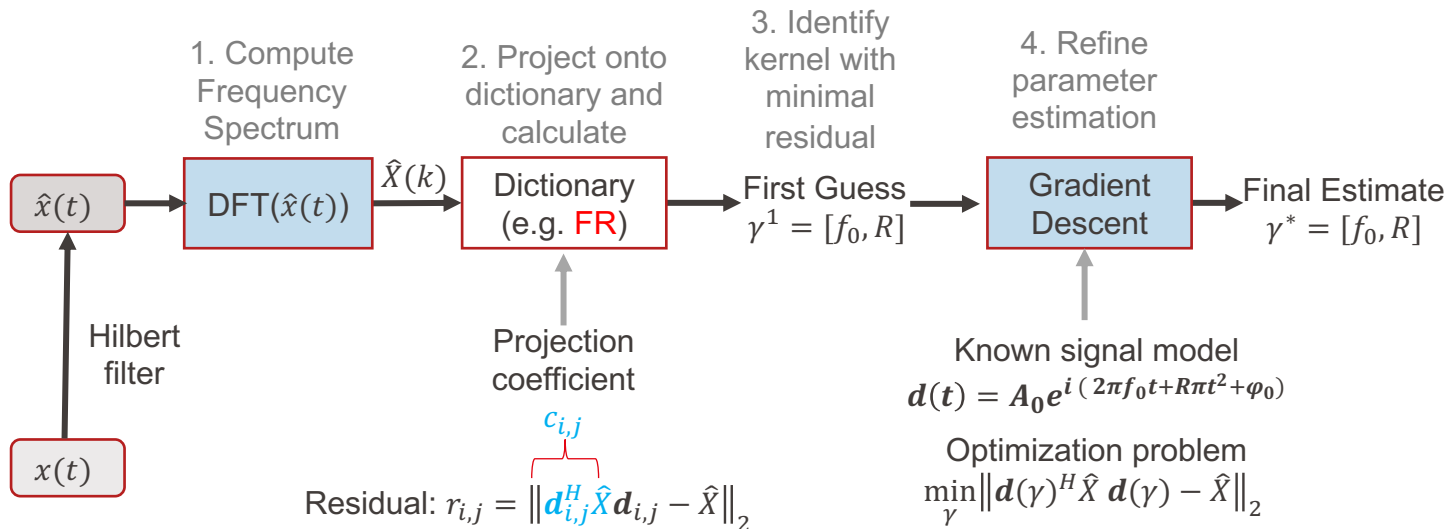
Functional Basis Analysis

- Parameter Identification



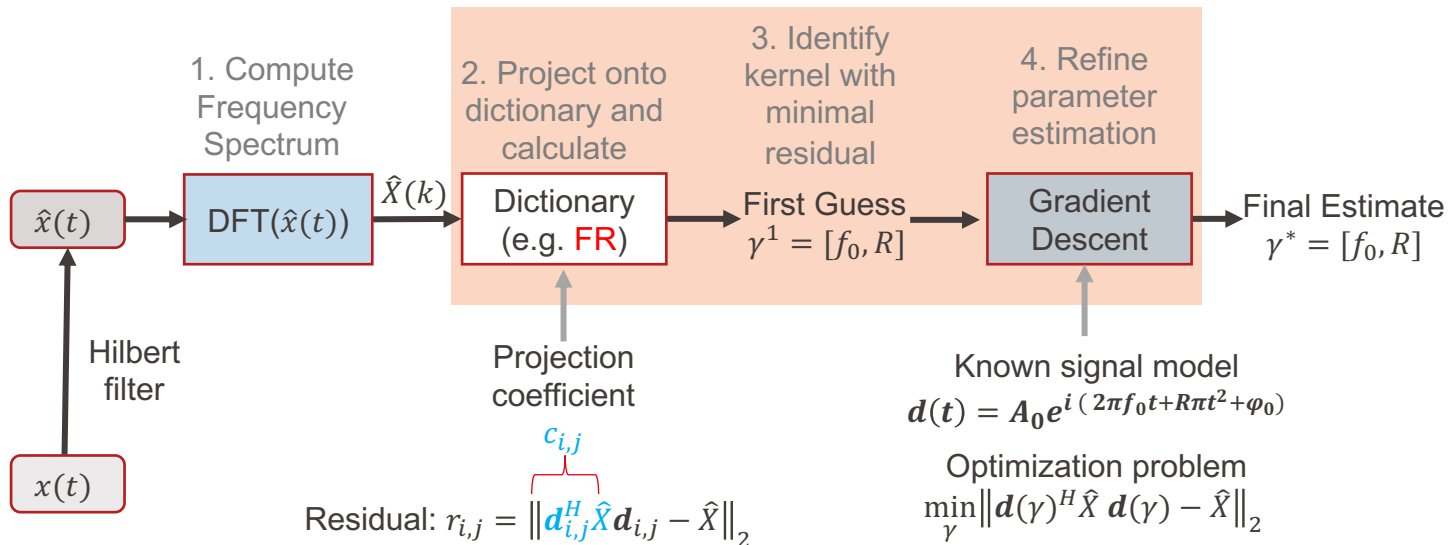
Functional Basis Analysis

- Parameter Identification



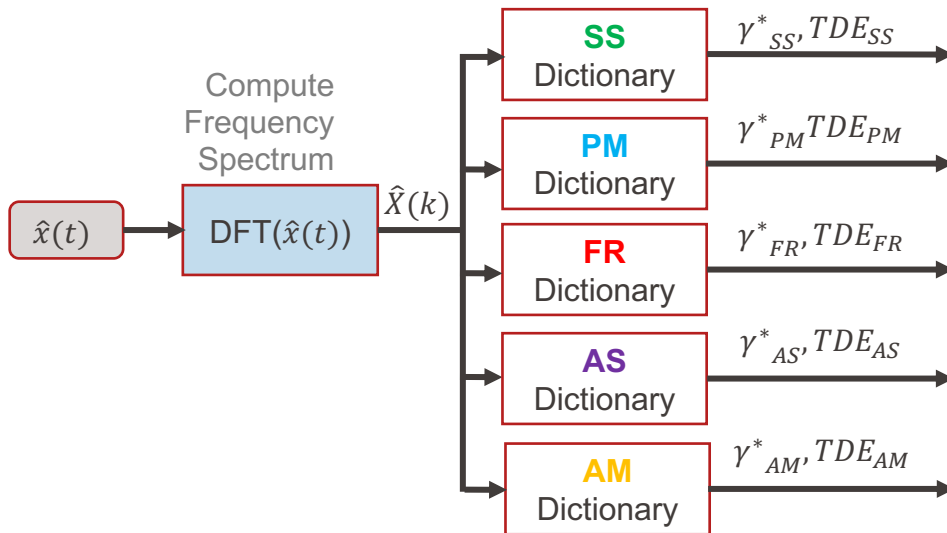
Functional Basis Analysis

- Parameter Identification



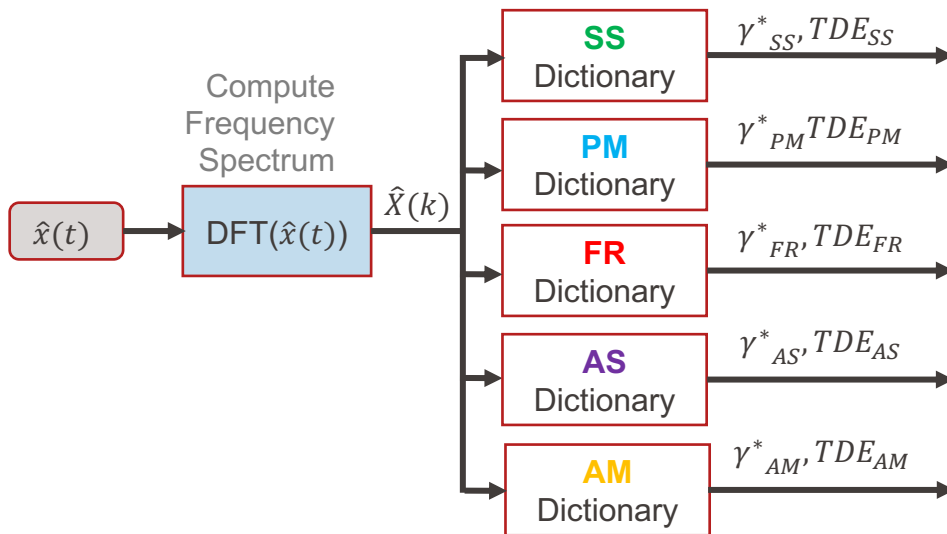
Functional Basis Analysis

- Dynamic Identification



Functional Basis Analysis

- Dynamic Identification



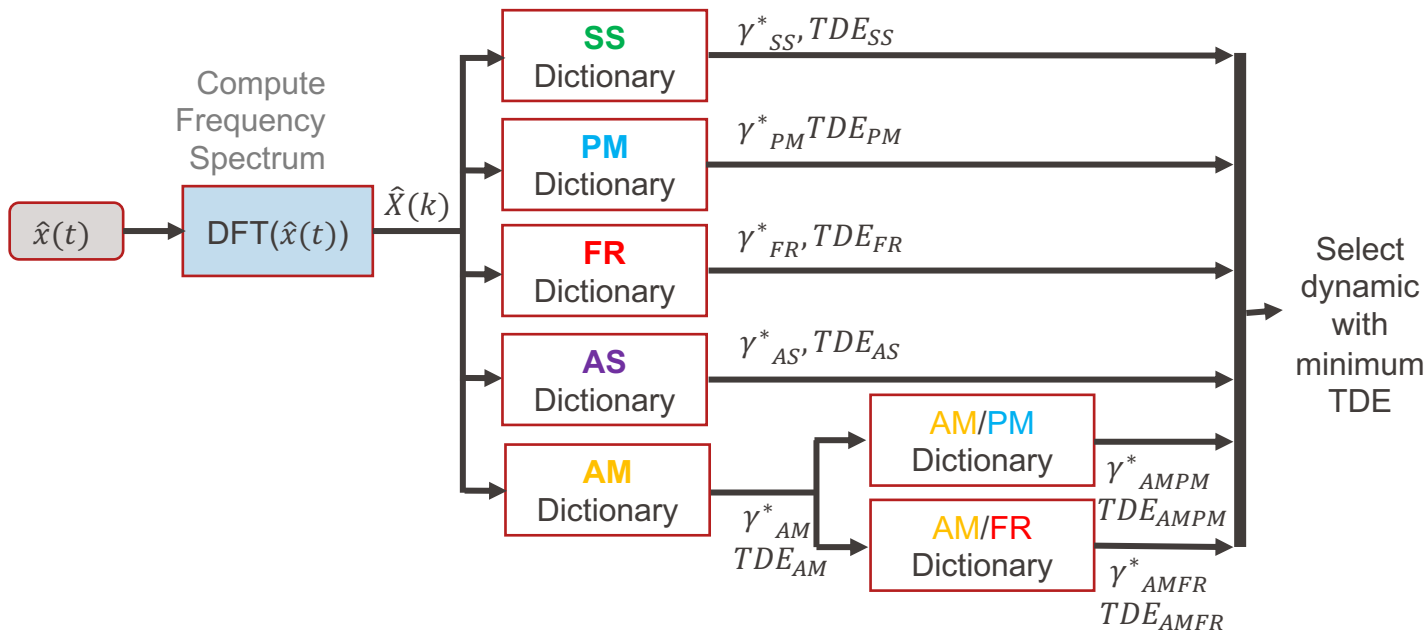
What about multi-dynamic signals?

AM/FR: $(1 + k_m \cos(2\pi f_m t + \varphi_m)) e^{i(2\pi f_0 t + R\pi t^2 + \varphi_0)}$

AM/PM: $(1 + k_m \cos(2\pi f_m t + \varphi_m)) e^{i(2\pi f_0 t + k_a \cos(2\pi f_a t + \varphi_a) + \varphi_0)}$

Functional Basis Analysis

- Dynamic Identification



Performance Evaluation

- Comparison made between:
 1. **FBA**
 2. **Static phasor method:**
 - 2-point iterative IpDFT method (i-*IpDFT*) [13]
 - Han window and negative spectrum compensation
 3. **Dynamic phasor method:**
 - Compressed Sensing Taylor-Fourier Multifrequency (CSTFM) method [7]
 - 1st and 2nd order derivatives approximated
 - Corrections made to static phasor parameters (f_0, A_0, φ_0)

M. Bertocco, G. Frigo, C. Narduzzi, C. Muscas, and P. A. Pegoraro, "Compressive sensing of a Taylor-Fourier multifrequency model for synchrophasor estimation," *IEEE Trans. on Instr. and Meas.*, vol. 64, no. 12, pp. 3274–3283, 2015.

A. Derviskadic, P. Romano, and M. Paolone, "Iterative-interpolated DFT for synchrophasor estimation: A single algorithm for P- and M-class compliant PMUs," *IEEE Trans. on Instr. and Meas.*, vol. 67, no. 3, pp.547–558, Mar. 2018

Performance Evaluation

■ Metrics:

- **Time Domain Error (TDE):** residuals of time-domain reconstruction

$$TDE = \frac{\|x_{est}(t_n) - x_{ref}(t_n)\|_2}{\sum_{n=1}^L |x_{ref}(t_n)|}$$

- **Frequency Error (FE):** comparing instantaneous frequency at the center of the window [14]

$$FE = \left| f\left(\frac{T_w}{2}\right) - f_{est}\left(\frac{T_w}{2}\right) \right|$$

- **Parameter Error:** parameter estimation error

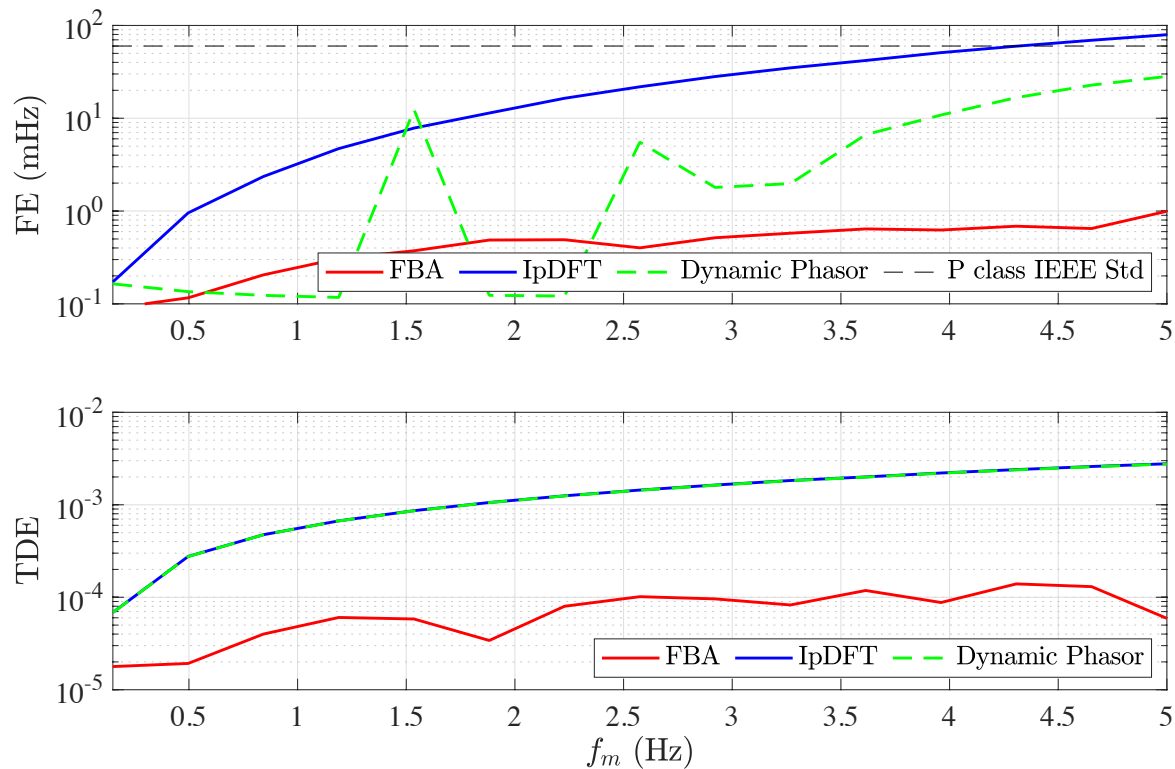
$$e.g., R \text{ error} = |R - R_{est}|$$

■ Tests:

- Synthetic signals created for each signal dynamic case
- 60 ms sliding window (50 fps)
- 80 dB Gaussian noise
- Tests based on IEEE C37.118 Standard [14]

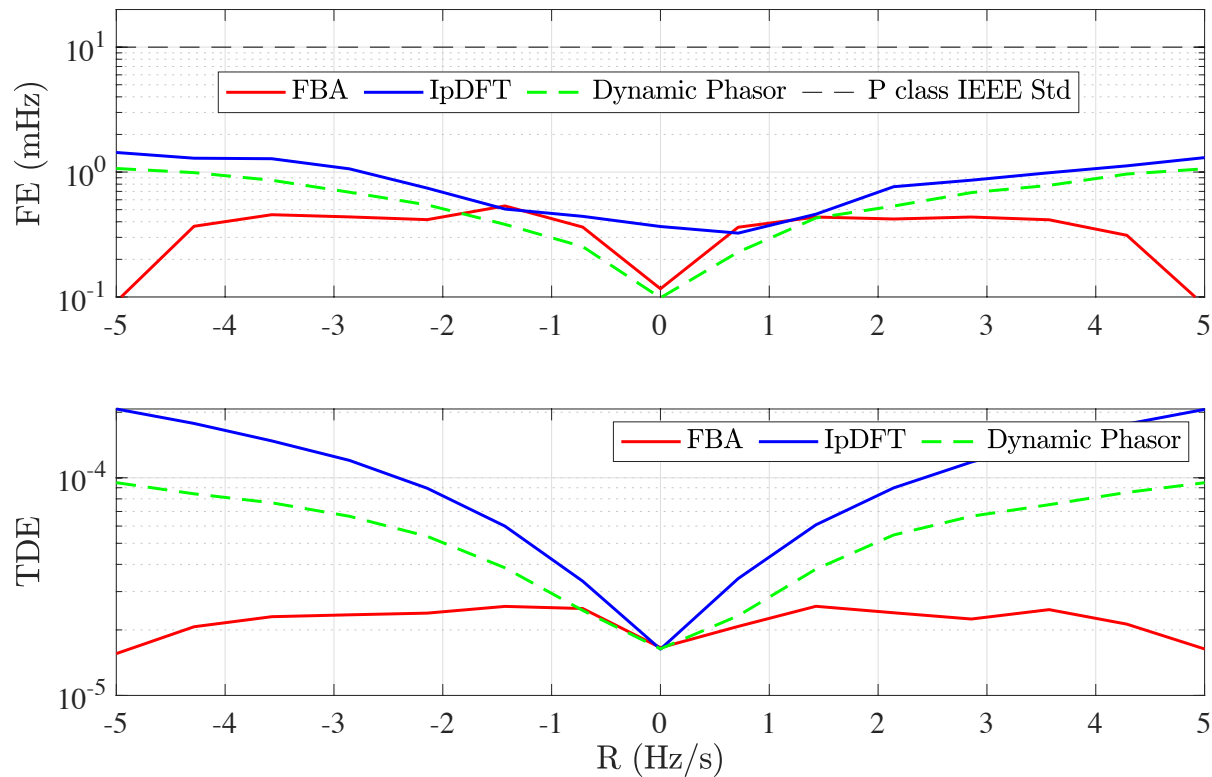
Amplitude Modulations

$$f_0 = 50.15 \text{ Hz}, k_m = 10\%, f_m = [0.1, 5] \text{ Hz}$$



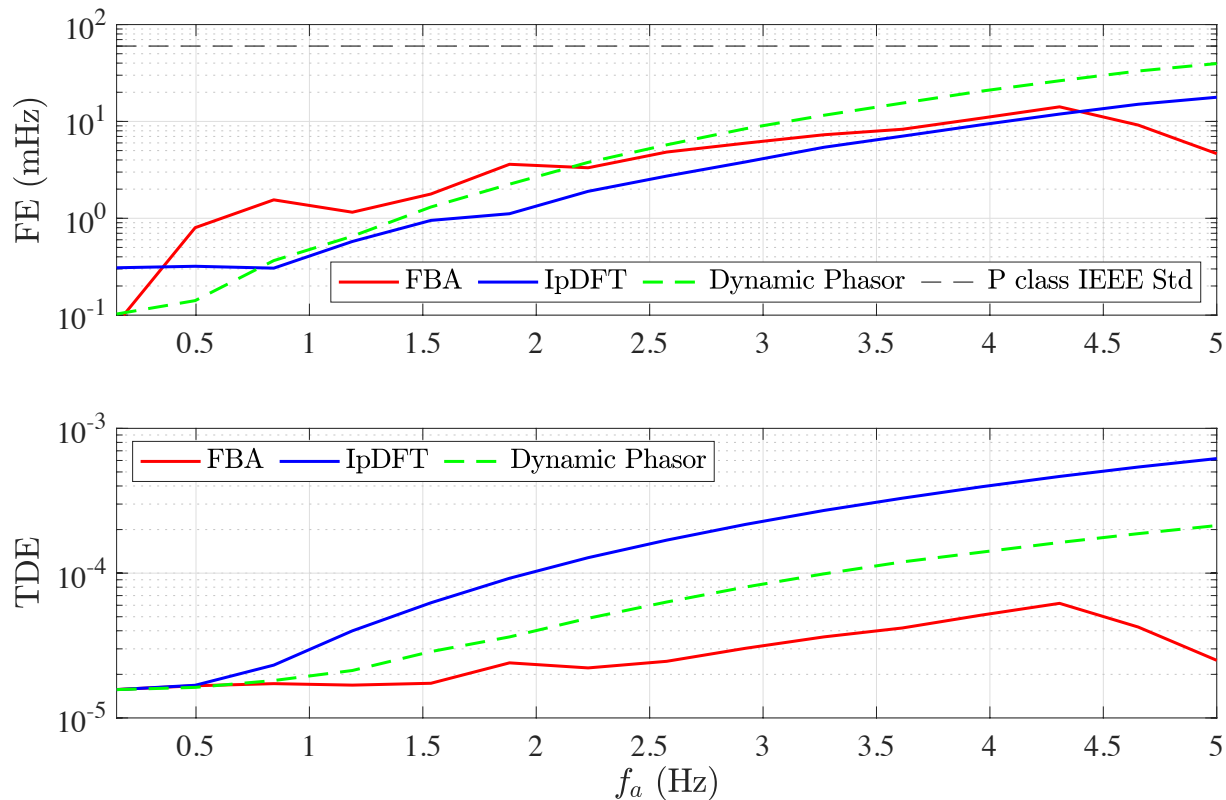
Frequency Ramps

$$f_0 = 50.15 \text{ Hz}, R = [-5, 5] \text{ Hz/s}$$



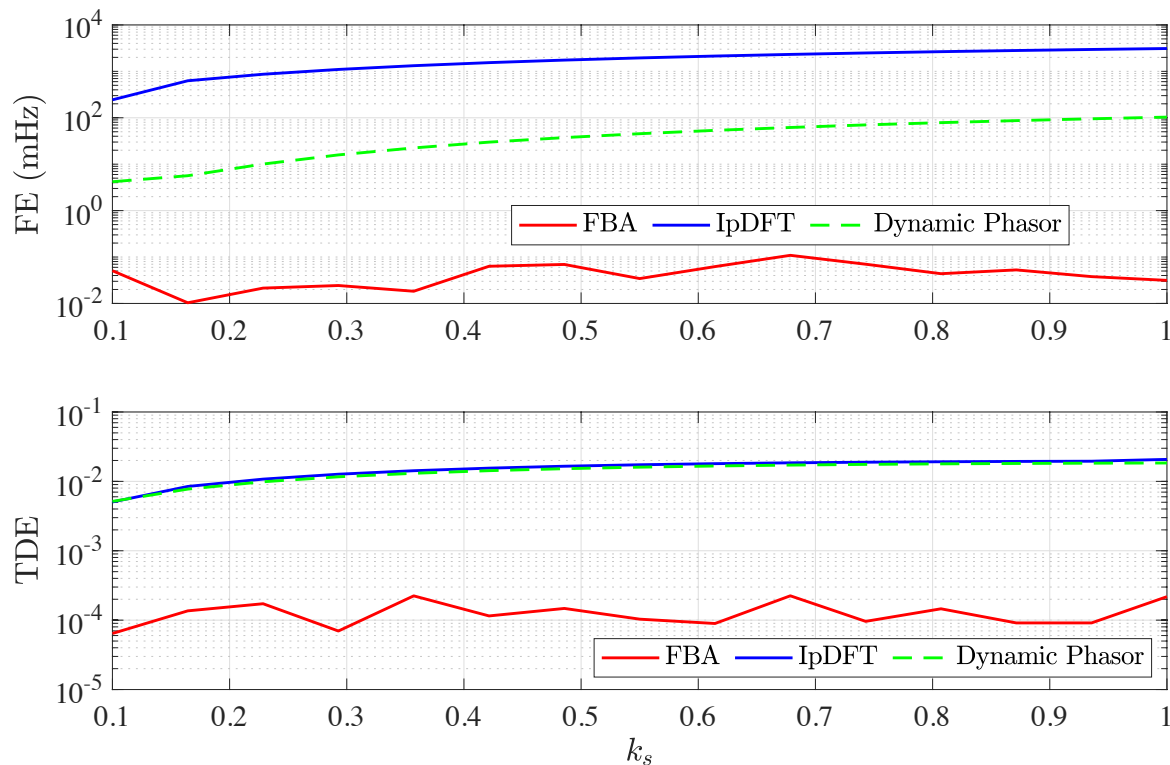
Phase Modulations

$$f_0 = 50.15 \text{ Hz}, k_a = 10\%, f_a = [0.1, 5] \text{ Hz}$$



Amplitude Steps

$$f_0 = 50\text{Hz}, k_s = [10, 100]\%$$

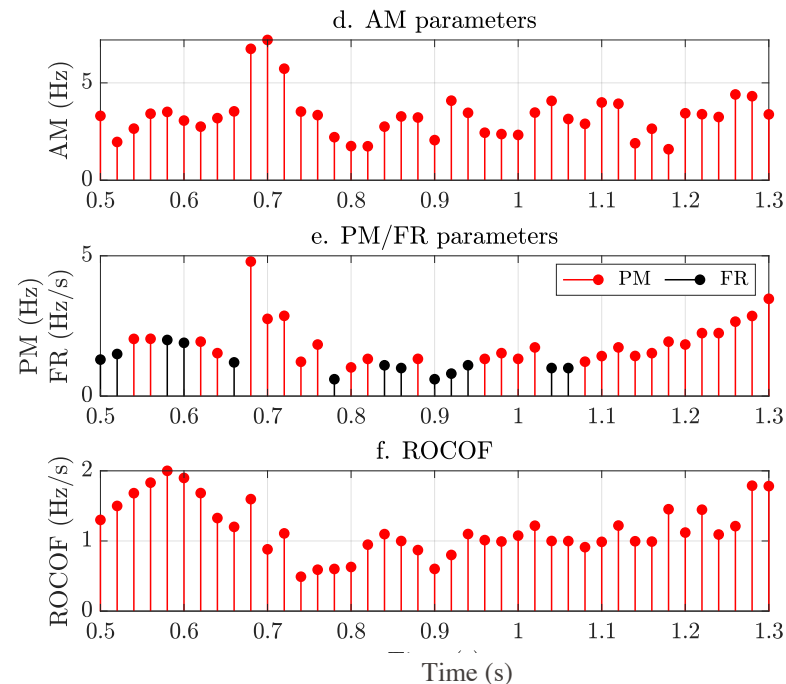
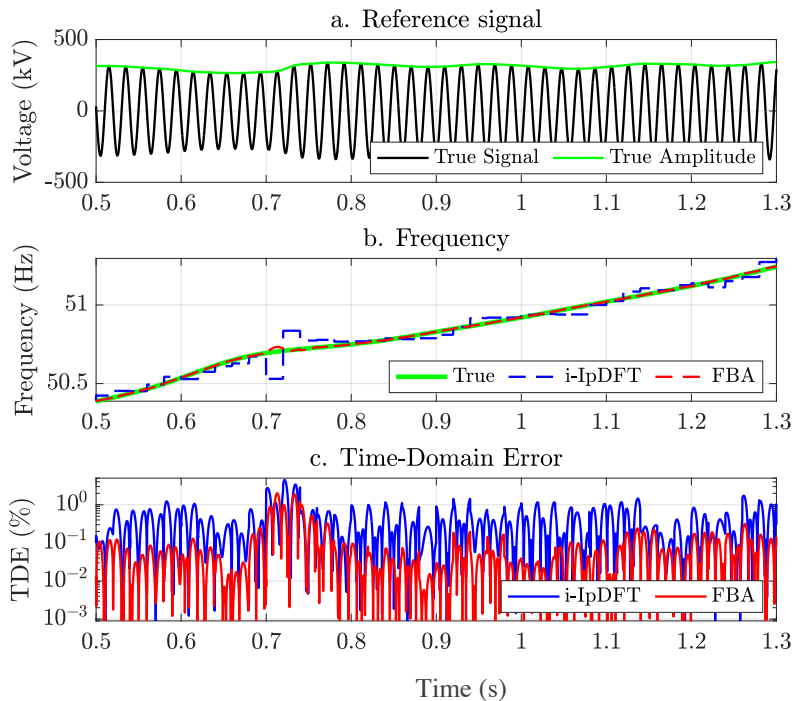


Parameters Errors

Dynamic	Max FE (mHz)			Max RFE (mHz/s)			Mean TDE	
	60 ms	200 ms	IEEE Limit	60 ms	200 ms	IEEE Limit	60 ms	200 ms
SS	0.1	1.6E-2	5	2	1.2	10	8.2E-06	4.5E-06
AM	0.9	0.1	60	32	6	2300	9.9E-6	5.7E-06
FR	5	4.7	10	147	222	400	1E-05	1.8E-05
PM	8	13	60	112	420	2300	1.3E-05	2.4E-05
AS	4	1.3		27	108		1.1e-03	5.2E-04
AM/FR	2	3		223	196		1.4E-05	3.7E-05
AM/PM	8	18	60	276	498	3000	1.9E-5	3.7E-05
Dynamic	Mean Parameter Error for 200 ms window							
	f_0 (mHz)	f_m (mHz)	φ_m (rad)	f_a (mHz)	φ_a (rad)	R (mHz/s)	k_s (%)	t_s (ms)
SS	0.2							
AM	0.2	3.5	0.018					
FR	5					48		
PM	14			58	0.16			
AS	1						2.6	1.5
AM/FR	4	45	0.078			30		
AM/PM	13	39	0.04	76	0.14			

Real-World Examples

Blackout in Turkey, 2015 [17]

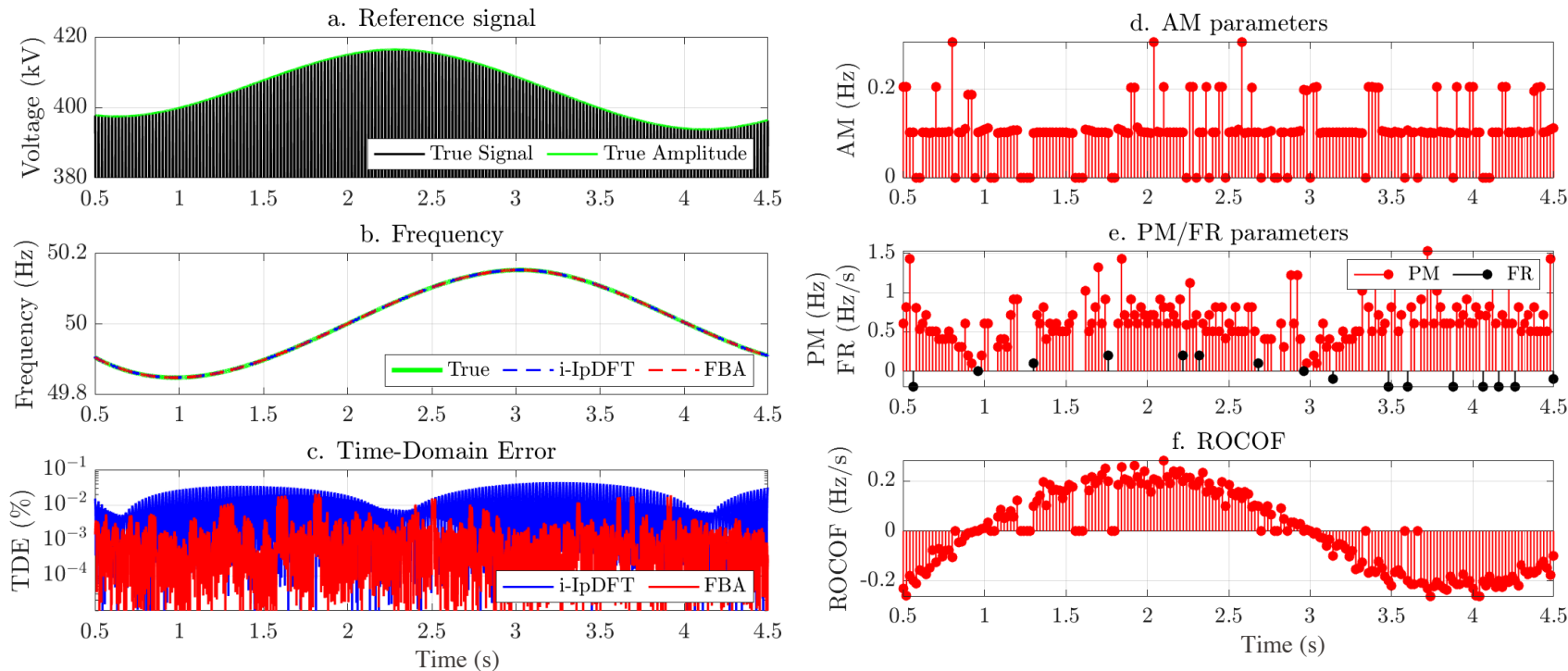


A. Karpilow, A. Derviskadic, G. Frigo, M. Paolone. "Characterization of Real-World Power System Signals in Non-Stationary Conditions using a Dictionary Approach" [Accepted] PowerTech Conference, Madrid, Spain, 2021.

ENTSO-E, "Report on blackout in turkey on 31st march 2015 – final version 1.0," European Network of Transmission System Operators for Electricity, Project Group Turkey, Tech. Rep., 2015

Real-World Examples

- Inter-area oscillations in Central Europe, 2017 [13]



A. Karpilow, A. Derviskadic, G. Frigo, M. Paolone. "Characterization of Real-World Power System Signals in Non-Stationary Conditions using a Dictionary Approach" [Accepted] PowerTech Conference, Madrid, Spain, 2021.
 ENTSO-E, "Oscillation Event 03.12.2017," 2018.

HT applied to Elementary Circuit Theory

Resistance

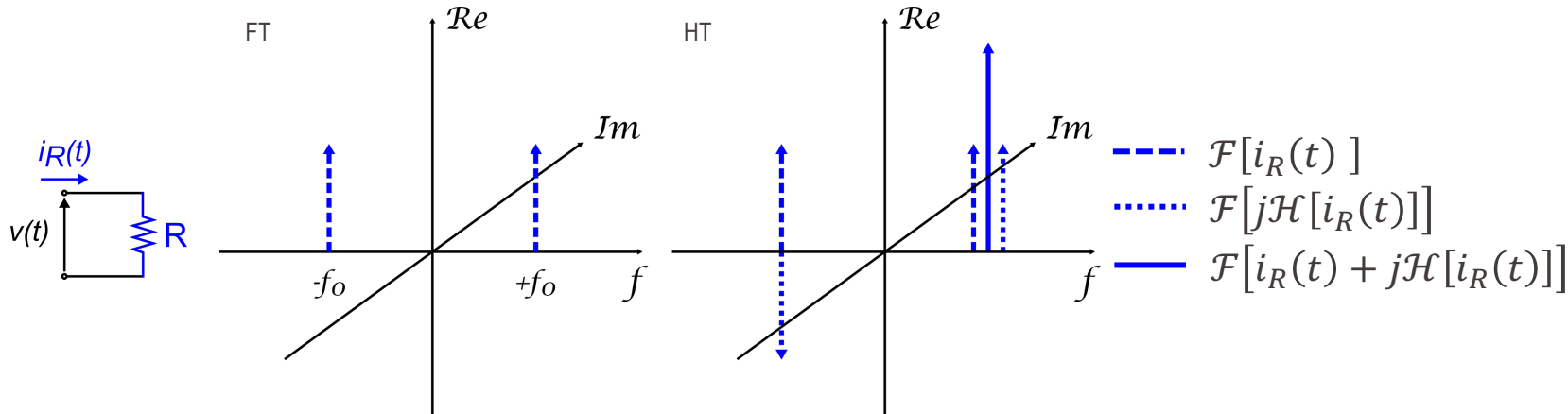
$$v(t) = V \cos(\omega_0 t) \rightarrow i_R(t) = \frac{v(t)}{R} = I_R \cos(\omega_0 t)$$

FT

$$\mathcal{F}[i_R(t)] = \frac{I_R}{2} \cdot [\delta(\omega - \omega_0) + \delta(\omega + \omega_0)]$$

HT

$$\hat{i}_R(t) = I_R \cdot [\cos(\omega_0 t) + j \sin(\omega_0 t)] = I_R e^{j\omega_0 t}$$



HT applied to Elementary Circuit Theory

Inductance

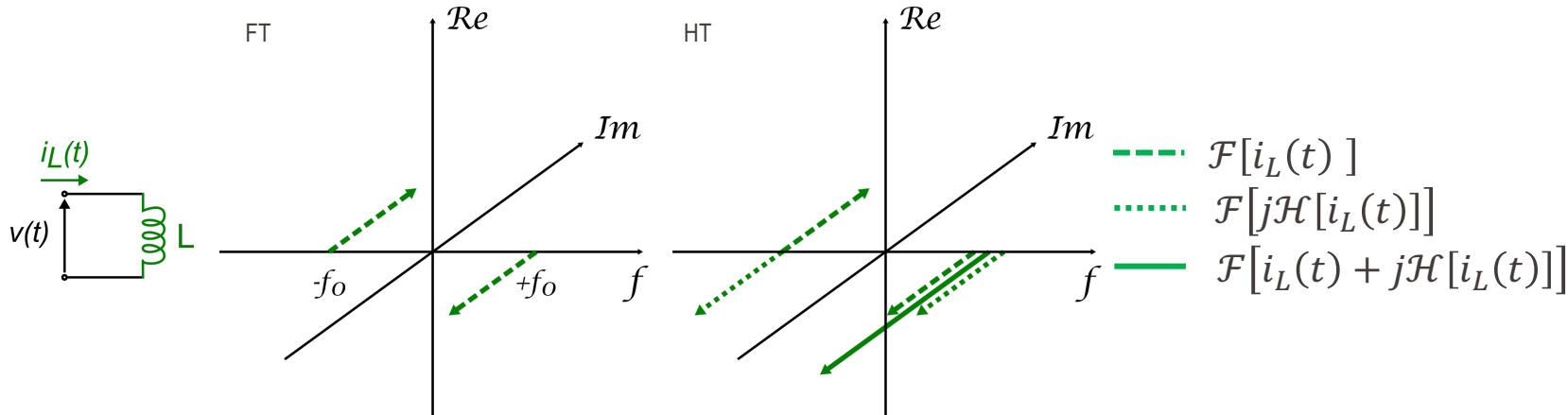
$$v(t) = V \cos(\omega_0 t) \rightarrow i_L(t) = \int \frac{di_L(t)}{dt} = \int \frac{v(t)}{L} = I_L \sin(\omega_0 t)$$

FT

$$\mathcal{F}[i_L(t)] = -j \cdot \frac{I_L}{2} \cdot [\delta(\omega - \omega_0) - \delta(\omega + \omega_0)]$$

HT

$$\hat{i}_L(t) = I_L \cdot [\sin(\omega_0 t) - j \cos(\omega_0 t)] = -j \cdot I_L e^{j\omega_0 t}$$



HT applied to Elementary Circuit Theory

Capacitance

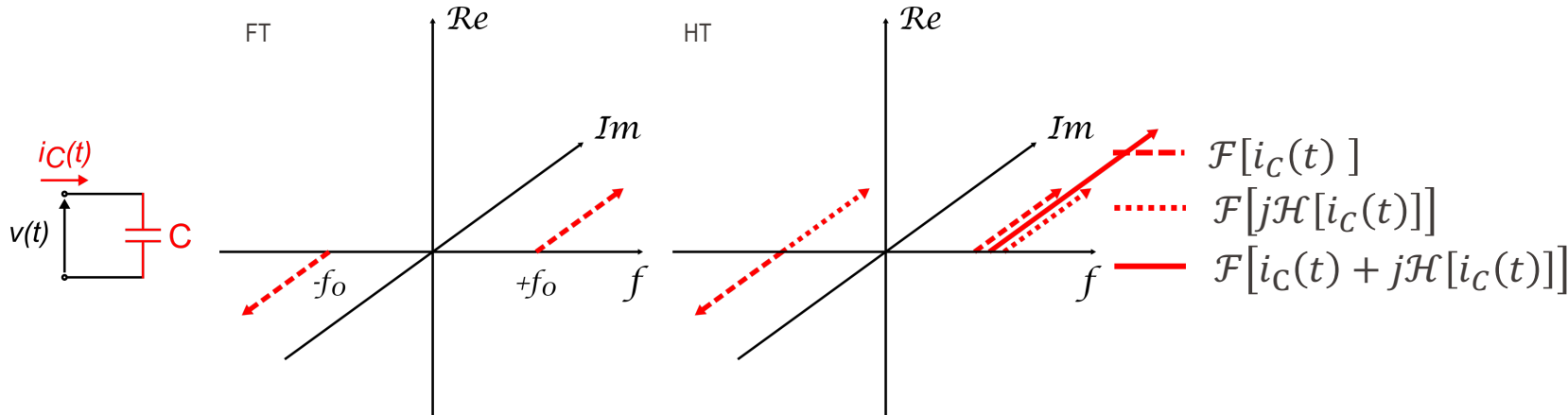
$$v(t) = V \cos(\omega_0 t) \rightarrow i_C(t) = C \frac{di_C(t)}{dt} = -I_C \sin(\omega_0 t)$$

FT

$$\mathcal{F}[i_C(t)] = j \cdot \frac{I_C}{2} \cdot [\delta(\omega - \omega_0) - \delta(\omega + \omega_0)]$$

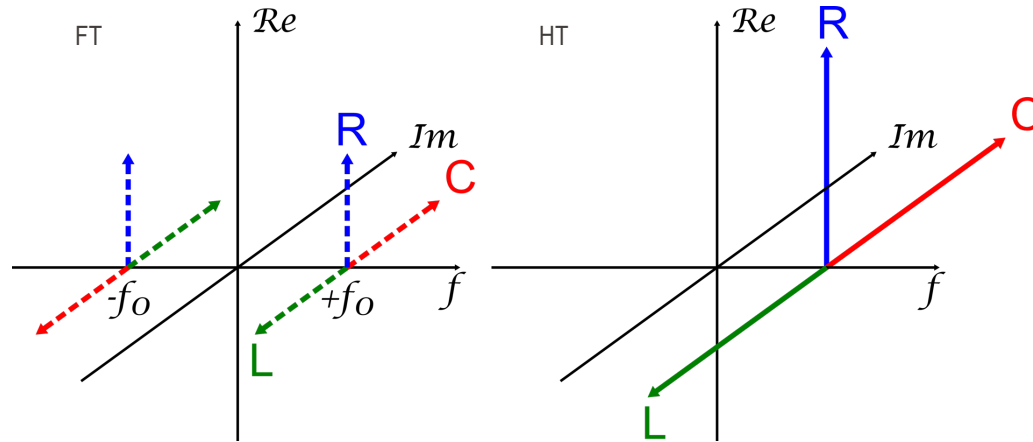
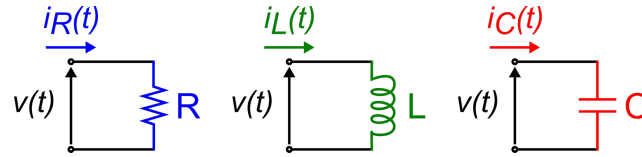
HT

$$\hat{i}_C(t) = -I_C \cdot [-\sin(\omega_0 t) + j \cos(\omega_0 t)] = j \cdot I_C e^{j\omega_0 t}$$



HT applied to Elementary Circuit Theory

The HT representation of a generic resistor, inductor or capacitor consists only of positive frequency components → New way to formulate Kirchhoff's circuit laws using HT



Conclusions

- Recent events in low-inertia power systems have shown how the use of phasors may lead to large approximations when modelling signals of electrical quantities of reduced-inertia power grids.
- Dynamic phasors outperform stationary phasors in dynamic conditions but still rely on narrow-band approximations of signals and cannot represent in a complete way signals characterized by a continuous spectrum.
- The HT, integrated with the analytical signal representation, may be the appropriate tool for modelling broad-band signals associated to inertia-less power system dynamics.
- The presentation has shown how the functional basis analysis (FBA) allows for the extraction of signal parameters and the identification of common dynamics.
- The FBA method demonstrated improved performance for common signal dynamics and real-world signals when compared to dynamic and static phasor methods.

References

- [1] M. Yaghoobi, L. Duadet, M. E. Davies, "Parametric Dictionary Design for Sparse Coding," IEEE Trans. on Signal Processing, vol. 57, no. 12, 2009.
- [2] IEEE Standard for Synchrophasor Measurements for Power Systems, "IEEE Std C37.118.1-2011 (Revision of IEEE Std C37.118-2005), pp.1–61, Dec 2011.
- [3] D. Petri, D. Fontanelli and D. Macii, "A Frequency-Domain Algorithm for Dynamic Synchrophasor and Frequency Estimation," in IEEE Transactions on Instrumentation and Measurement, vol. 63, no. 10, pp. 2330-2340, Oct. 2014.
- [4] P. Romano and M. Paolone, "Enhanced Interpolated-DFT for Synchrophasor Estimation in FPGAs: Theory, Implementation, and Validation of a PMU Prototype," in IEEE Transactions on Instrumentation and Measurement, vol. 63, no. 12, pp. 2824-2836, Dec. 2014.
- [5] P. Banerjee and S. C. Srivastava, "An Effective Dynamic Current Phasor Estimator for Synchrophasor Measurements," in IEEE Transactions on Instrumentation and Measurement, vol. 64, no. 3, pp. 625-637, March 2015.
- [6] D. Belega, D. Fontanelli and D. Petri, "Dynamic Phasor and Frequency Measurements by an Improved Taylor Weighted Least Squares Algorithm," in IEEE Transactions on Instrumentation and Measurement, vol. 64, no. 8, pp. 2165-2178, Aug. 2015.
- [7] M. Bertocco, G. Frigo, C. Narduzzi, C. Muscas and P. A. Pegoraro, "Compressive Sensing of a Taylor-Fourier Multifrequency Model for Synchrophasor Estimation," in IEEE Transactions on Instrumentation and Measurement, vol. 64, no. 12, pp. 3274-3283, Dec. 2015.

References

- [8] ENTSO-E, “Report on blackout in turkey on 31st March 2015 – final version 1.0,” European Network of Transmission System Operators for Electricity, Project Group Turkey, Tech. Rep., 2015.
- [9] G. Frigo et al, "Definition of Accurate Reference Synchrophasors for Static and Dynamic Characterization of PMUs," in IEEE Transactions on Instrumentation and Measurement, vol. 66, no. 9, pp. 2233-2246, Sept. 2017.
- [10] AEMO, “Review of the Black System South Australia report system event of 28 September 2016,” Australian Energy Market Operator, Tech. Rep., 2017.
- [11] NERC, "1,200 MW fault induced solar photovoltaic resource interruption disturbance report," NERC, Atlanta, GA, 2017.
- [12] A. Derviskadic, P. Romano, and M. Paolone, “Iterative-interpolated DFT for synchrophasor estimation: A single algorithm for P- and M-class compliant PMUs,” IEEE Trans. on Instr. and Meas., vol. 67, no. 3, pp.547–558, Mar. 2018.
- [13] ENTSO-E, “Oscillation Event 03.12.2017,” 2018.
- [14] C. Narduzzi, M. Bertocco, G. Frigo and G. Giorgi, "Fast-TFM—Multifrequency Phasor Measurement for Distribution Networks," in IEEE Transactions on Instrumentation and Measurement, vol. 67, no. 8, pp. 1825-1835, Aug. 2018.
- [15] A. Derviškadić, “Synchronized Sensing for Wide-Area Situational Awareness of Electrical Grids in Non-Stationary Operating Conditions,” EPFL PhD Thesis, 2019.
- [16] A. Derviškadić, G. Frigo and M. Paolone, "Beyond Phasors: Modeling of Power System Signals Using the Hilbert Transform," in IEEE Transactions on Power Systems, vol. 35, no. 4, pp. 2971-2980, July 2020.

References

- [17] M. Paolone, T. Gaunt, X. Guillaud, et al, “Fundamentals of power systems modelling in the presence of converter-interfaced generation,” *Electric Power Systems Research*, vol. 189, 2020.
- [18] A. Karpilow, A. Derviskadic, G. Frigo, M. Paolone, “Characterization of Non-Stationary Signals in Electric Grids: a Functional Dictionary Approach” (under review). *IEEE Transactions on Power Systems*, 2021.
- [19] A. Karpilow, A. Derviskadic, G. Frigo, M. Paolone, “Characterization of Real-World Power System Signals in Non-Stationary Conditions using a Dictionary Approach”. *PowerTech 2021*, Madrid.
- [20] A. Karpilow, A. Derviškić, G. Frigo, M. Paolone, “Step detection in power system waveforms for improved RoCoF and frequency estimation, *Electric Power Systems Research*, vol. 212, 2022, 108527.
- [21] A. Karpilow, M. Paolone, A. Derviškić and G. Frigo, "Step Change Detection for Improved ROCOF Evaluation of Power System Waveforms," 2022 International Conference on Smart Grid Synchronized Measurements and Analytics (SGSMA), 2022.